Inorg. Chem. **2002**, *41*, 4859–4871

Cobalt(II) and Cobalt(III) Dipicolinate Complexes: Solid State, Solution, and in Vivo Insulin-like Properties

Luqin Yang,[†,‡] Debbie C. Crans,*[,‡] Susie M. Miller,[‡] Agnete la Cour,[‡] Oren P. Anderson,[‡] Peter M. Kaszynski,[§] Michael E. Godzala, III,[§] LaTanya D. Austin,[§] and Gail R. Willsky[§]

Department of Chemistry, College of Natural Sciences, Colorado State University, Fort Collins, Colorado 80523-1872, and Department of Biochemistry, University at Buffalo School of Medicine and Biomedical Sciences, 140 Farber Hall, Buffalo, New York 14214

Received January 22, 2002

The synthesis and characterization of Co(II) and Co(III) 2,6-pyridinedicarboxylate (dipic^{2-}) complexes are reported. Solid-state X-ray characterizations were performed on $[Co(H_2dipic)(dipic)]\cdot 3H_2O$ and $[Co(dipic)(\mu\text{-dipic})Co(H_2O)_5]\cdot 2H_2O$. Two coordination modes not previously observed in dipicolinate transition metal complexes were observed in these complexes; one involves metal coordination to the short C–O (C═O) bond, and the other involves metal coordination to a protonated oxygen atom. Solution studies, including paramagnetic NMR and UV–vis spectroscopy, were done showing the high stability and low lability of the Co(III) complex, whereas the Co(II) complexes exhibited ligand exchange in the presence of excess ligand. The $[Co(dipic)_2]^{2-}$ complex has pH dependent lability and in this regard is most similar to the $[VO_2dipic]^-$ complex. The $[Co(dipic)_2]^{2-}$ was found to be effective in reducing the hyperlipidemia of diabetes using oral administration in drinking water in rats with STZ-induced diabetes. Oral administration of $VOSO_4$ was used as a positive control for metal efficacy against diabetes. In addition to providing a framework to evaluate structure–function relationships of various transition metal complexes in alleviating the symptoms of diabetes, this work describes novel aspects of structural and solution cobalt chemistry.

Introduction

The coordination chemistry of cobalt has been important in biology mainly because of coenzyme B_{12}. A recent report of insulin-like action of cobalt chloride[1] implies that such metal compounds may have similarities with vanadium compounds, which for two decades have been known to exhibit insulin-like effects.[2−5] Recently, we have undertaken an exhaustive comparison of transition metal complexes' solid-state and solution chemistry as well as their insulin-like effects. To this end, we have synthesized several complexes from Co(II) or (III) and dipicolinate and studied their solid-state and aqueous solution properties. Cobalt dipicolinate complexes[6−13] have been known for more than 30 years, but no X-ray and solution characterizations have been reported.[14] One of our complexes, $[Co(dipic)_2]^{2-}$, on

* To whom correspondence should be addressed. E-mail: crans@lamar.colostate.edu. Phone: (970) 491-7635. Fax: (970) 491-1801.

† Permanent address: Department of Chemistry, Peking University, Beijing, China.

‡ Colorado State University.

§ University at Buffalo School of Medicine and Biomedical Sciences.

(1) (a) Saker, F.; Ybarra, J.; Leahy, P.; Hanson, R. W.; Kalhan, S. C., Ismail-Beigi, F. *Am. J. Physiol.* **1998**, *274*, E984-E991. (b) Ybarra, J.; Behrooz, A.; Gabriel, A.; Koseoglu, M. H.; Ismail-Beigi, F. *Mol. Cell. Endocrinol.* **1997**, *133*, 151−160.

(2) (a) Yuen, V. G.; Orvig, C.; McNeill, J. H. *Can J. Physiol. Pharmacol*. **1993**, *71*, 263−269. (b) Fujimoto, S.; Fujii, D.; Yasui, H.; Matsushita, R.; Takada, J.; Sakurai, H. *J. Clin. Biochem. Nutr*. **1997**, *23*, 113−129. (c) Cohen, N.; Halberstam, M.; Shlimovich, P.; Chang, C. J.; Shamoon, H.; Rossetti L. *J. Clin. Invest.* **1995**, *95*, 2501−2509. (d) Golfine, A. B.; Patti, M.-E.; Zuberi, L.; Goldstein, B. J.; LeBlanc, R.; Landaker, E. J.; Jiang, A. Y.; Willsky, G. R.; Kahn, C. R. *Metab., Clin. Exp.* **2000**, *49*, 400−401.

(3) (a) Greco, D. S.; Crans, D. C. *J. Inorg. Biochem.*, under revision. (b) Crans, D. C. *J. Inorg. Biochem.* **2000**, *80*, 123−131.

(4) Tracey, A. S.; Crans, D. C. *Vanadium Compounds. Chemistry, Biochemistry, and Therapeutic Applications*; ACS Symposium Series 711; American Chemical Society: Washington, DC, 1998.

(5) Crans, D. C.; Yang, L.; Jakusch, T.; Kiss, T. *Inorg. Chem.* **2000**, *39*, 4409−4416.

(6) Hernandez-Molina, R.; Fedin, V. P.; Sokolov, M. N.; Saysell, D. M.; Sykes, A. G. *Inorg. Chem.* **1998**, *37*, 4328−4334.

(7) Saysell, D. M.; Sykes, A. G. *Inorg. Chem.* **1996**, *35*, 5536−5539.

(8) Saysell, C. G.; Borman, C. D.; Baron, A. J.; McPherson, M. J.; Sykes, A. G. *Inorg. Chem.* **1997**, *36*, 4520−4525.

(9) Mauk, A. G.; Coyle, C. L.; Bordignon, E.; Gray, H. B. *J. Am. Chem. Soc.* **1979**, *101*, 5054−5056.

(10) Mauk, A. G.; Bordignon, E.; Gray, H. B. *J. Am. Chem. Soc.* **1982**, *104*, 7654−7657.

(11) Nathan, L. C.; Zapien, D. C.; Mooring, A. M.; Doyle, C. A.; Brown, J. A. *Polyhedron* **1989**, *8*, 745−748.

(12) Hoof, D. L.; Walton, R. A. *Inorg. Chim. Acta* **1975**, *12*, 71−78.

(13) Matthews, R. W.; Hamer, A. D.; Hoof, D. L.; Tisley, D. G.; Walton, R. A. *J. Chem. Soc., Dalton Trans.* **1973**, 1035−1038.

10.1021/ic020062l CCC: $22.00
Published on Web 08/23/2002

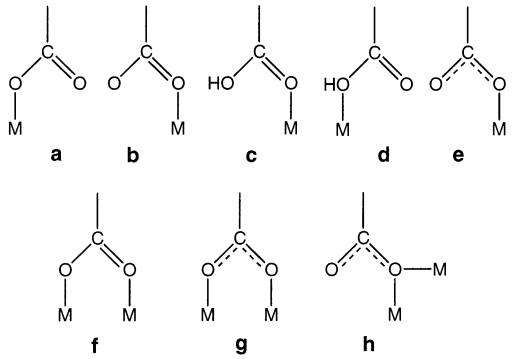

Figure 1. Coordination modes for metal−carboxylate complexes. The coordination modes previously reported are labeled a,[15−22] c,[15−24] e,[19,22,24] f,[21] g,[18] and h.[20] Coordination modes b and d are reported here.

the basis of similarities in solution properties with $[VO_2dipic]^-$, was selected for evaluation of insulin-like effects in STZ-induced diabetic rats. Ultimately, understanding the differences in insulin-like effects of these two transition metal complexes and their mode of action as insulin-mimetic agents requires a detailed understanding of the chemical properties of the corresponding cobalt and vanadium complexes.

Preparation and studies of both Co(II) and Co(III) 1:2 complexes ($[Co(dipic)_2]^-$,[9] $[Co(dipic)_2]^{2-}$,[11] and ($[Co(Hdipic)_2]$)[12,13] have been reported as well as the preparation of a 1:1 Co(II) complex (Co(dipic)).[13] A range of different coordination modes exists in transition metal−dipicolinate complexes[15−24] depending on whether the anionic or protonated forms of $dipic^{2-}$ are coordinated to the metal ion (Figure 1, coordination modes a−h). In this study, two new coordination types have been observed, one which involves metal coordination to the short C−O (C═O) bond (b) and the other which involves metal coordination to the protonated oxygen atom (d). The structures of the Co−dipicolinate complexes were found to be different than known Ni−dipicolinate complexes and be similar to known Cu−dipicolinate complexes. The Co(III) complex, $[Co(dipic)_2]^-$, is used as a reference compound in some electron-transfer reactions[6−10] although characterization of this cobalt complex has been limited to the solid state.[11−13] The assumption that the solid-state species persists in solution is well founded on the literature reports regarding solution properties of related cobalt complexes,[6−13] and accordingly, our studies show an unexpected rich speciation chemistry. We report paramagnetic 2D exchange spectroscopy (EXSY) NMR solution studies of the cobalt complex, to obtain a detailed understanding of the solution species, their protonation states, and their labilities. These studies show that the Co(II) complexes are labile and that this lability is pH dependent.

The effect of oral administration of one cobalt compound ($K_2[Co(dipic)_2]$) was tested in rats with STZ-induced diabetes. Although $K_2[Co(dipic)_2]$ only had a limited effect on hyperglycemia, it lowered both the elevated levels of serum cholesterol and triglyceride in these rats. Information on the insulin-mimetic effect of well characterized compounds is important to understand the mode of action of transition metal complexes in alleviating diabetes. This paper provides some information on the insulin-mimetic action of $K_2[Co(dipic)_2]$, and comparing this information with the effect of corresponding vanadium complexes will eventually lead to a better understanding of how such complexes work. The complexes that form between cobalt and dipicolinate are compared to other transition metal complexes characterized by X-ray crystallography, IR, visible absorption, and NMR spectroscopy.[25−30] Collectively, these studies have led to discoveries of new coordination modes and solution chemistry of these cobalt dipicolinate complexes.

Experimental Section

Materials and General Methods. All reagents used were of reagent grade. The water was distilled and deionized in an ion-exchange column. $VOSO_2 \cdot 5H_2O$ was purchased from Aldrich Chemical Co. $K_3Co(CO_3)_3 \cdot 4H_2O$ was prepared following the method described for $Na_3Co(CO_3)_3 \cdot 3H_2O$,[31] and the content of water molecules was determined by TGA. TGA was performed on a TGA 2950 thermogravimetric analyzer. UV−vis absorption spectra were recorded on a Perkin-Elmer Lambda 4B spectrophotometer. IR spectra of KBr pellets were recorded on a Perkin-Elmer 1600 FT-IR spectrometer.

Preparation of Complexes. K[Co(dipic)$_2$] (1). $K_3Co(CO_3)_3 \cdot 4H_2O$ (0.980 g, 2.30 mmol) was added slowly to a stirred water slurry of H_2dipic at pH 3.2 (0.840 g, 5.00 mmol) at ambient temperature. The pH of the solution was adjusted to 6.4 with K_2CO_3. After addition of 30% H_2O_2 (1 mL), the resulting solution was stirred overnight. The solid was collected by filtration and washed with water followed by ethanol. The red solid product, 0.302 g, was obtained in 30.7% yield. IR (KBr, cm^{-1}): 3449 (m), 3085 (w, ν(C−H)), 3054 (w, ν(C−H)), 1664 (vs), 1649 (vs, $\nu(CO_2^-)$), 1474 (w), 1333 (s, $\nu(CO_2^-)$), 1182 (m), 1166 (m), 1105 (m), 919

(14) Crystallographic studies were reported for the related bis(picolinate) complex, although these authors refer to this complex as a dipicolinic acid complex. Lumme, P.; Viertola, R.; Lindgren, G. *Suomen Kemistil.* **1969**, *42B*, 270−273.
(15) Quaglieri, P. P.; Loiseleur, H.; Germaine, T. *Acta Crystallogr.* **1972**, *B28*, 2583−2590.
(16) Gaw, H.; Robinson, W. R.; Walton, R. A. *Inorg. Nucl. Chem. Lett.* **1971**, *7*, 695−699.
(17) Chiesi Villa, A.; Guastini, C.; Musatti, A.; Nardelli, M. *Gazz. Chim. Ital.* **1972**, *102*, 226−233.
(18) Hakansson, K.; Lindahl, M.; Svensson, G.; Albertsson, J. *Acta Chem. Scand.* **1993**, *47*, 449−455.
(19) Okabe, N.; Oya, N. *Acta Crystallogr.* **2000**, 305−307.
(20) Laine, P.; Gourdon, A.; Launay, J.-P.; Tuchagues, J.-P. *Inorg. Chem.* **1995**, *34*, 5150−5155.
(21) Laine, P.; Gourdon, A.; Launay, J.-P. *Inorg. Chem.* **1995**, *34*, 5138−5149.
(22) Biagini-Cingi, M.; Chiesi Villa, A.; Guastini, C.; Nardelli, M. *Gazz. Chim. Ital.* **1971**, *101*, 825−832.
(23) Biagini-Cingi, M.; Chiese Villa, A.; Guastini, C.; Nardelli, M. *Gazz. Chim. Ital.* **1972**, *102*, 1026−1033.
(24) Drew, M. G. B.; Matthews, R. W.; Walton, R. A. *J. Chem. Soc. A* **1970**, 1405−1410.
(25) Bothner-By, A. A.; Domaille, P. J.; Gayathri, C. *J. Am. Chem. Soc.* **1981**, *103*, 5602−5603.
(26) Stephan, M.; Muller, P.; Zenneck, U.; Pritzkow, H.; Siebert, W.; Grimes, R. N. *Inorg. Chem.* **1995**, *34*, 2058−2067.
(27) Attar, S.; Balch, A. L.; Van Calcar, P. M.; Winkler, K. *J. Am. Chem. Soc.* **1997**, *119*, 3317−3323.
(28) Pulici, M.; Caneva, E.; Crippa, S. *J. Chem. Res., Synop.* **1997**, 160−161.
(29) Koerner, R.; Olmstead, M. M.; Van Calcar, P. M.; Winkler, K.; Balch, A. L. *Inorg. Chem.* **1998**, *37*, 982−988.
(30) Fox, O. D.; Leung, J. F.-Y.; Hunter, J. M.; Dalley, N. K.; Harrison, R. G. *Inorg. Chem.* **2000**, *39*, 783−390.
(31) Bauer, H. F.; Drinkard, W. C. *J. Am. Chem. Soc.* **1960**, *82*, 5031−5032.

(m), 872 (w), 858 (w), 820 (w), 780 (m), 750 (m), 710 (w), 679 (m), 600 (w), 487 (m). ^{1}H NMR (D_2O, DSS): 8.8 (t, 1 H, p-H), 8.6 (d, 2 H, m-H) ppm. UV−vis (H_2O): 511 nm (ϵ 672 $M^{-1}cm^{-1}$) [lit.: 513 nm, ϵ 653 M^{-1} cm^{-1},[35] 510 nm, ϵ 630 M^{-1} cm^{-1})].[9] Anal. Calcd for C_{14} $H_6N_2O_8CoK$: C, 39.25; H, 1.40; N, 6.54. Found: C, 39.36; H, 1.32; N, 6.65.

K_2[Co(dipic)$_2$]·7H_2O (2). K_2CO_3 (1.38 g, 10.0 mmol) was added slowly to a turbid aqueous solution containing H_2dipic (1.67 g, 10.0 mmol) and $CoCl_2$·6H_2O (1.19 g, 5.00 mmol) with stirring. When kept at 80−90 °C for 1−2 h, the solution changed from purple to brown. After standing at ambient temperature overnight, a deep purple-brown crystalline solid precipitated from the solution. The crystalline solid was filtered off, washed with water, and dried in air. This solid was found to be [Co(II)(dipic)(μ-dipic)Co(II)(H_2O)$_5$]·2H_2O (see later). The resulting filtrate was concentrated to about 20 mL and kept at ambient temperature for several hours before a deep grayish-brown crystalline solid was precipitated. The solid was collected, washed with water, and dried in air. A total of 1.63 g K_2[Co(dipic)$_2$]·7H_2O was obtained with a yield of 55.0%. IR (KBr, cm^{-1}): 3447 (vs, br), 3089 (w, ν(C−H)), 1644 (vs, ν(CO_2^-)) 1422 (s), 1373 (vs, ν(CO_2^-)), 1278 (s), 1185 (s), 1079 (s), 1035 (s), 915 (s), 826 (s), 769 (s), 741 (m), 694 (m), 674 (m), 538 (w), 469 (w). ^{1}H NMR (D_2O): 92 (s, m-H), 31 (s, p-H) ppm (19 °C). UV−vis (H_2O, d−d): 583 (ϵ 16.8 M^{-1} cm^{-1}), 531 (ϵ 12.0 M^{-1} cm^{-1}), 460 nm (ϵ 17.5 M^{-1} cm^{-1}). TGA: 50−100 °C, weight lost 18.6% (calcd for 6 H_2O 18.2%), complex decomposed at 460 °C. Anal. Calcd for $C_{14}H_{20}N_2O_{15}CoK_2$: C, 28.33; H, 3.39; N, 4.72. Found: C, 28.25; H, 2.97; N, 4.86.

Alternatively, the complex K_2[Co(dipic)$_2$]·7H_2O can be obtained from solutions with pH values above 8. From solutions with high pH, the yields are consistently >90%. The $Co(OOCCH_3)_2$·4H_2O salt can be used as a Co(II) precursor.

[Co(II)(dipic)(μ-dipic)Co(II)(H_2O)$_5$]·2H_2O (4). This purple complex was isolated as the first product during the preparation of K_2[Co(dipic)$_2$]·7H_2O at neutral or acidic pH. The amount of isolated product was 0.525 g, corresponding to a yield of 34.7% (based on $CoCl_2$·6H_2O). The structure of the complex was determined by X-ray diffraction. IR (KBr, cm^{-1}): 3478 (vs, br), 3239 (vs, br), 1618 (vs, ν(CO_2^-)) 1430 (s), 1386 (vs, ν(CO_2^-)), 1286 (s), 1118 (m), 1077 (m), 1037 (m), 765 (m), 734 (w), 694 (w), 678(w), 600 (w), 544 (w), 489 (w). ^{1}H NMR (D_2O): 102.5, 92.3 (s, m-H), 37.3, 30.5 (s, p-H) ppm (19 °C). Anal. Calcd for $C_{14}H_{20}N_2O_{15}Co$: C, 29.27; H, 3.48; N, 4.88. Found: C, 29.31; H, 3.32; N, 4.96.

Reacting $CoCl_2$ with H_2dipic can also generate this complex in solutions in the range pH 2−5 as long as the stoichiometries of metal to ligand range from 1:1 to 4:1. The yields of such reactions are above 90% and clearly are the method of choice for preparation of this 1:1 complex.

[Co(II)(H_2dipic)(dipic)]·3H_2O (3). Solid $CoCl_2$·6H_2O (0.24 g, 1.0 mmol) was added to a hot (70−90 °C) stirred water solution (20−50 mL) containing H_2dipic (0.34 g, 2.0 mmol). After heating for 1−2 h, the purple solution was cooled and kept at ambient temperature overnight. Deep red-purple crystals of [Co(II)(H_2dipic)-(dipic)]·3H_2O were formed. The crystals were collected, washed with water, and dried in air. The 0.215 g obtained corresponds to a 47.5% yield. The crystal structure was determined by X-ray diffraction. IR (KBr, cm^{-1}): 3397 (vs), 3256 (sh), 3100 (w), 1700 (sh), 1620 (vs, ν(CO_2^-)), 1593 (s), 1439 (m), 1396 (sh), 1381 (s), 1367 (s, ν(CO_2^-)), 1286 (s), 1079 (s), 1036 (m), 911 (m), 768 (s), 720 (br, m), 691 (m), 678 (m), 538 (m). ^{1}H NMR (D_2O): 102, 92 (broad), 31 (broad) ppm (19 °C). Anal. Calcd for $C_{14}H_{14}N_2O_{11}Co$: C, 37.75; H, 3.15; N, 6.29. Found: C, 37.82; H, 3.00; N, 6.39.

Co(dipic)·3.5H_2O (5). This complex was obtained as a minor side product from the reaction generating [Co(II)(H_2dipic)(dipic)]·3H_2O. The deep purple crystals of ([Co(II)(H_2dipic)(dipic)]·3H_2O) were separated first, after which slow evaporation for several days at ambient temperature gave a solid precipitate from the almost evaporated light purple-pink solution. The solid was a light purple powder. IR (KBr, cm^{-1}): 3511 (w, sh), 3422 (w, br), 3222 (w), 3111 (vw), 3067 (w), 2833 (w, br), 2700 (vw), 1686 (vs, ν(CO_2^-)), 1639 (s), 1612 (w), 1597 (w), 1576 (vw), 1459 (m), 1405 (m), 1396 (s), 1348 (w), 1330 (m), 1289 (m), 1257 (s, ν(CO_2^-)), 1178 (w), 1163 (w), 1085 (m), 1031 (m), 998 (m), 906 (m), 855 (m), 798 (w), 771 (w), 753 (m), 702 (s), 669 (w), 648 (m), 586 (w), 535 (w). ^{1}H NMR (D_2O): 102 (broad), 37 (broad) ppm (19 °C). Anal. Calcd for $C_7H_{10}NO_{7.5}Co$: C, 29.27; H, 3.48; N, 4.88. Found: C, 29.16; H, 2.72; N, 4.94.

Alternatively, the 1:1 compound could be prepared as follows. A hot aqueous solution of H_2dipic (0.34 g, 2.0 mmol) was added slowly with stirring to an aqueous solution containing $CoCl_2$·6H_2O (0.48 g, 2.0 mmol). The volume of the resulting purple mixture was about 40 mL, and it was kept at ambient temperature overnight. A total of 0.157 g (35.3% yield based on H_2dipic) of deep red-purple crystals of [Co(II)(H_2dipic)(dipic)]·3H_2O were obtained (confirmed by ^{1}H NMR). The solution was evaporated at ambient temperature for several days resulting in an additional 0.43 g of a light purple solid (yield 74.9% based on H_2dipic). The ^{1}H NMR spectrum verified that the light purple solid was mainly the 1:1 complex; however, this solid presumably also contains a small amount of $CoCl_2$.

X-ray Crystallography. X-ray diffraction data were recorded on a Bruker AXS SMART CCD diffractometer employing Mo Kα radiation (graphite monochromator). Crystallographic results and other details are listed in Table 1. An absorption correction was applied by using SADABS.[32a] Structures were solved by direct methods and refined (on F^2, using all data) by a full-matrix, weighted least-squares process. Anisotropic displacement parameters were used to refine all non-hydrogen atoms. All hydrogen atoms (except H(40A) and H(40B) which belong to a disordered water molecule in the [Co(II)(H_2dipic)(dipic)]·3H_2O complex) were found in the electron density map and refined isotropically. H40A and H40B were placed in idealized positions relative to the major component of the disordered water oxygen atom, O40A. Standard Bruker control (SMART) and integration (SAINT) software was employed, and Bruker SHELXTL[32b] software was used for structure solution, refinement, and graphics.

Sample Preparation for NMR Studies. The samples for spectral analysis were generally prepared by dissolving the crystalline complexes (and ligand where appropriate) in deuterium oxide. When necessary, the pH was adjusted with a stock solution of DCl or NaOD.

1D NMR Spectroscopy. 1D ^{1}H and ^{13}C spectra were recorded on a Varian INOVA-300 spectrometer (7.0 T) at 300 MHz for ^{1}H and 75.5 MHz for ^{13}C. The paramagnetic ^{1}H spectra were acquired with a 51020 Hz spectral window, pulse widths of 60°−90°, and acquisition times of 0.08−1.67 s with no relaxation delay. A 2 Hz exponential line broadening was applied prior to Fourier transfor-

(32) (a) Sheldrick, G. M. *SADABS (a Program for Siemens Area Detection Absorption Correction)*; University of Göttingen: Göttingen, Germany, 1999. (b) Sheldrick, G. M. *SHEXTL, Siemens Analytical X-ray Diffraction*; Siemens: Madison, WI, 1996; Vol. 5.
(33) Crans, D. C.; Boukhobza, I. *J. Am. Chem. Soc.* **1998**, *120*, 8069−8078.
(34) Johnson, T. M.; Meisler, M. H.; Bennett, M. I.; Willsky, G. R. *Diabetes*, **1990**, *39*, 757−759.
(35) Casellato, U.; Graziani, R.; Bonomo, R. P.; Di Bilio, A. *J. Chem. Soc.* **1991**, 23−31.

Table 1. Crystallographic Data for [Co(II)(H_2dipic)(dipic)]·3H_2O (**3**) and [Co(II)(dipic)(μ-dipic)Co(II)(H_2O)$_5$]·2H_2O (**4**)

	3	**4**
empirical formula	$C_{14}H_{14}CoN_2O_{11}$	$C_{14}H_{20}N_2Co_2O_{15}$
fw	445.20	574.18
cryst size/mm^3	0.21 × 0.22 × 0.38	0.10 × 0.30 × 0.45
cryst syst	monoclinic	monoclinic
space group	$P2_1/c$	$P2_1/c$
a/Å	13.806(3)	8.4106(1)
b/Å	10.036(2)	27.3392(3)
c/Å	13.646(3)	9.6301(1)
β/°	115.81(3)	98.188(1)
Z	4	4
V/Å^3	1702.1(6)	2191.76(4)
d (calcd)/Mg/m^3	1.737	1.740
F(000)	908	1168
abs coeff/mm^{-1}	1.075	1.591
temp/K	169(2)	167(2)
λ/Å	0.71073	0.71073
θ/deg	$1.64 \le \theta \le 28.35$	$1.49 \le \theta \le 28.27$
h	$-17 \le h \le 18$	$-5 \le h \le 11$
k	$-13 \le k \le 7$	$-34 \le k \le 36$
l	$-18 \le l \le 18$	$-12 \le l \le 12$
reflns collected	10959	14354
independent reflns	4114	5252
R_{int}	0.0686	0.0485
data/restraints/params	4114/1/310	5252/0/379
R [$I > 2\sigma(I)$]	R1 = 0.0497	R1 = 0.0285
	wR2 = 0.0895	wR2 = 0.0627
R (all data)	R1 = 0.1282	R1 = 0.0400
	wR2 = 0.1174	wR2 = 0.0658
$\Delta\rho_{max,min}$/e Å^{-3}	0.387, −0.645	0.385, −0.735

mation. DSS (3-(trimethylsilyl)propane sulfonic acid sodium salt) was used as an external reference for both ^{1}H and ^{13}C chemical shifts. The paramagnetic ^{13}C NMR were recorded with spectral windows of 90600−150900 Hz, a 90° pulse width, an acquisition time of 0.5 s, 0.0−0.3 s relaxation delays, and three different decoupling settings. Initial spectra were recorded using no decoupling, and then the Waltz-16 program was used with a bandwidth of 4−5 kHz and selection at the frequency of H2 (6961 Hz) and H1/H3 (25916 Hz), respectively. A 10 Hz exponential line broadening was applied prior to Fourier transformation.

Variable temperature ^{1}H NMR spectra were also recorded. The temperature for the variable temperature experiments was calibrated using an 80% ethylene glycol sample in DMSO-d_6 to an accuracy of ±2 °C.[33] The NMR spectra were recorded first at room temperature, at gradually increasing temperatures, and finally again at ambient temperature.

2D EXSY NMR Spectroscopy. 2D homonuclear EXSY experiments were run on a Varian INOVA-300 spectrometer (7.0 T) at 300 MHz for ^{1}H at 75.5 MHz for ^{13}C. The 2D paramagnetic ^{1}H EXSY spectra shown in this work were recorded with sweep widths of 32895−39000 Hz, accumulation times of 0.15−0.249 s, delay times of 0.01−0.3 s, mixing times of 0.015−0.8 s, and 128 increments of 4−32 scans each. The narrow spectral window was chosen to increase sensitivity, and only the signal region of interest was included. This reduced the size of the data matrix required in the F1 domain and decreased accumulation times.

Animal Protocol. Modifications of the previously published procedure for the induction of diabetes and animal care were used.[34] Diabetes was induced in male Wistar rats weighing 182−218 g by injection of freshly prepared streptozotocin (60 mg/mL) in 0.9% saline at a dose of 60 mg/kg body weight by intraperitoneal or intravenous injection. Blood glucose levels were determined 4 days after streptozotocin injection with an Accucheck blood glucose monitor as previously published.[34] The diabetic animals were randomly assigned to the treated or to the untreated group. Normal untreated animals were matched in age and weight. Treatment consisted of daily adding $VOSO_4$ (0.78 mg/mL (3.1 mM) for days 1−14) or $[Co(dipic)_2]^{2-}$ (0.50 mg/mL (0.84 mM) for days 1−3 and 0.60 mg/mL (1.01 mM) for days 4−14). The amounts of compound were calculated including 7 water hydrates for $K_2[Co(dipic)_2]$ and 5 for $VOSO_4$. The treatment group $[Co(dipic)_2]^{2-}$ contained 8 animals, the $VOSO_4$ treated control group 7 animals, and the diabetic control group 5 animals, while 2 normal rats were used in this experiment. Data for the 2 normal animals were therefore supplemented with data for 1 animal used in another similar experiment for analysis of blood glucose and lipids (see later). Any animal appearing to be dehydrated, as monitored by loss of weight or physical examination, was rehydrated subcutaneously with 10−30 mL/day of lactated Ringer's bicarbonate solution (0.84%). Blood glucose levels were determined twice a week and urine ketones and glucose determined once a week using Ketodiastix. In the initial 2 week treatment period, no animals were removed from the experiment because of extreme dehydration or diarrhea.

To examine serum lipid levels at a time when both elevated triglyceride and cholesterol could be observed in the diabetic animals, the experiment was carried out for 4 weeks. Treatment for days 1−14 were as described. Treatment for days 15−28 consisted of daily adding $VOSO_4$ (1.6 mg/mL (6.2 mM) for days 15−28) or $[Co(dipic)_2]^{2-}$ (1.2 mg/mL (2.0 mM) for days 15−28) to the drinking water. Lipids were determined in serum obtained at sacrifice. Diabetic (4 of 4) and $[Co(dipic)_2]^{2-}$ treated (8 out of 8) animals were selected from this study for lipid analysis. The serum lipid data were supplemented with data from normal (4) and $VOSO_4$ (7) treated animals obtained from a similar set of animals examined in the experiment carried out at a different time. The data for these animals are included in Table 5. Triglyceride was determined using Sigma (St. Louis, Mo) Procedure No. 337, while cholesterol was determined using Sigma (St. Louis, Mo) Procedure No. 332.

Statistics. A one way ANOVA with Dunnett's multiple means test was used to analyze the animal data comparing all groups to the diabetic untreated group. The p values ≤ 0.05 were considered significant. Data are presented as the mean ± the standard error (SE).

Results and Discussion

Syntheses. Information regarding the preparation of complex ions $[Co(III)(dipic)_2]^-$, $[Co(II)(dipic)_2]^{2-}$, [Co(II)(dipic)·3H_2O], and [Co(II)(Hdipic)$_2$]·3H_2O[9,11,13,35] have been reported. The reported yields of the sodium salt and neutral complex ions range from 50% to 100%. In this work, we focused on preparation of K^+ salts. This salt was chosen because of the well-known fact that Na^+ and K^+ salts are innocuous and often are preferred countercations to use when it comes to administration of compounds to humans. Extending the reported method[35] to the preparation of the potassium salt ($K[Co(III)(dipic)_2]$) generated a mixture of Co(II) and Co(III) complexes at 70 °C, and in our hands, the addition of 3−4 equiv of oxidizing agent (H_2O_2) was necessary to isolate pure Co(III) complex. The preparation of the Co(II) complexes is pH sensitive, and pH values < 8 result in isolation of complexes with different stoichiometries.

The Co(III) complex could be prepared directly from $K_3Co(CO_3)_3$ and 2 equiv of H_2dipic at pH 6. $K_3Co(CO_3)_3$ was prepared with slight modification of the literature method.[31]

This preparation consistently gave low yields in our hands, and in order to obtain consistently high yields of the Co(III) complex, we added H_2O_2 to the reaction mixture. The K^+ salt of $[Co(II)(dipic)_2]^{2-}$ was prepared from $CoCl_2$ and 2 equiv of H_2dipic at a pH of about 9. These conditions gave the Co(II) complex in 90% yield and was the method used to prepare the material used in the solution studies. The protonated 1:2 complex ($[Co(II)(H_2dipic)(dipic)]\cdot 3H_2O$) was crystallized from solutions of 1 equiv of $CoCl_2$ and 2 equiv of H_2dipic at pH $\sim$ 1. The yield of this compound was only 30%−50% in our hands, significantly less than the yield reported in the literature.[13] The 1:1 complex was isolated from the described reaction mixture in 70% yield after standing at ambient temperature. On the basis of the elemental analysis and the characterization of this compound, it is also likely that the solid contains some $CoCl_2$.[36] But at low pH and ambient temperature, the major Co(II) complex isolated was Co(II)dipic$\cdot 3.5H_2O$. In contrast to the literature report,[13] attempts to prepare the 1:1 complex from solutions of 1 equiv of $CoCl_2$ or $Co(OAc)_2$ and 1 equiv of H_2dipic also resulted in some crystalline 1:2 protonated complex ($[Co(II)(H_2dipic)(dipic)]\cdot 3H_2O$) as the first precipitate. Attempts to prepare the 1:1 complex with an excess Co(II) starting material (1 to 4.5-fold excess) in the pH range 3−6 failed and resulted in crystalline 2:2 complex with yields >90%.

The novel 2:2 complex, $[Co(II)(dipic)(\mu\text{-dipic})Co(II)(H_2O)_5]\cdot 2H_2O$, was also isolated in crystalline form from reaction of $CoCl_2$ or $Co(AcO)_2$ and 2 equiv of H_2dipic at pH 3−6 in yields of 20%−40%. This 2:2 complex formed 1:1 and 1:2 species when dissolved in deuterium oxide.

Solid-State Characterization. Crystal Structure of $[Co(II)(H_2dipic)(dipic)]\cdot 3H_2O$ (3). The crystal data and selected bond distances and angles are shown in Tables 1 and 2, respectively. The molecular structure and atom labeling system is shown in Figure 2. Two nitrogen and four oxygen atoms are coordinated to the cobalt atom resulting in a distorted octahedron. Each of the two tridentate dipic ligands coordinates through two oxygen atoms and one nitrogen atom. One of the dipic groups is coordinated as $dipic^{2-}$ and the other as H_2dipic, resulting in this complex containing four of the different coordination modes (a−d) illustrated in Figure 1. The two Co−N bond distances are similar (2.017(3)−2.021(3) Å). Co−O bond distances range from 2.108(2) to 2.222(3) Å (average 2.166 Å). The longest bond is observed in a type c coordination mode (Co−O(2)), and the shortest bond is observed in a type a coordination mode (Co−O(12)). The carboxylate group C(6)O(1)O(3) is coordinated to cobalt by the coordination mode shown in d, and the carboxylate C(7)O(2)O(4) is coordinated to the cobalt by coordination mode c. The carboxylate groups C(16)O(11)O(13) and C(17)O(12)O(14) are coordinated to the cobalt in coordination modes b and a, respectively. The identification of both a fully protonated neutral H_2dipic and a dianionic $dipic^{2-}$ ligand in $[Co(II)(H_2dipic)(dipic)]$ distinguishes this structure from that of the nickel complex, $[Ni(Hdipic)_2]\cdot 3H_2O$, which contained two monoprotonated $Hdipic^-$ ligands.[15−17] The structure of $[Co(II)(H_2dipic)(dipic)]$ exhibits some similarities with the structures of a silver(II)

(36) On the basis of characterization by ^{1}H NMR and IR spectroscopy, no excess dipic is present in solution. Furthermore, the elemental analysis obtained support the presence of some $CoCl_2$ in Co(dipic)$\cdot 2H_2O$. According to the elemental analysis, this material contains 0.2 equiv of $CoCl_2$ when prepared at larger scales (Calcd: C, 29.37; H, 2.45; N, 4.90).

Table 2. Selected Bond Distances (Å) and Bond Angles (deg) for $[Co(II)(H_2Dipic)(dipic)]\cdot 3H_2O$ (**3**) and $[Co(II)(dipic)(\mu\text{-dipic})Co(II)(H_2O)_5]\cdot 2H_2O$ (**4**)

	3	**4**
Co(1)−N(1)	2.021(3)	2.026(2)
Co(1)−N(11)	2.017(3)	2.033(1)
Co(1)−O(1)	2.137(3)	2.186(1)
Co(1)−O(2)	2.222(3)	2.123(1)
Co(1)−O(11)	2.195(2)	2.193(1)
Co(1)−O(12)	2.108(2)	2.225(1)
C(6)−O(1)	1.292(4)	1.277(2)
C(6)−O(3)	1.227(4)	1.249(2)
C(7)−O(2)	1.241(4)	1.273(2)
C(7)−O(4)	1.288(4)	1.256(2)
C(16)−O(11)	1.261(4)	1.268(2)
C(16)−O(13)	1.270(4)	1.252(2)
C(17)−O(12)	1.271(4)	1.273(2)
C(17)−O(14)	1.247(4)	1.254(2)
Co(2)−O(14)		2.097(1)
Co(2)−O(21)		2.180(1)
Co(2)−O(22)		2.090(1)
Co(2)−O(23)		2.062(1)
Co(2)−O(24)		2.060(2)
Co(2)−O(25)		2.094(1)
N(11)−Co(1)−N(1)	173.6(1)	172.00(5)
N(11)−Co(1)−O(1)	101.2(1)	103.99(5)
N(11)−Co(1)−O(2)	106.0(1)	104.94(5)
N(11)−Co(1)−O(12)	77.2(1)	76.19(5)
N(11)−Co(1)−O(11)	75.7(1)	75.53(5)
N(1)−Co(1)−O(1)	76.9(1)	75.74(5)
N(1)−Co(1)−O(2)	75.2(1)	76.66(5)
N(1)−Co(1)−O(12)	109.1(1)	95.87(5)
N(1)−Co(1)−O(11)	98.0(1)	112.46(5)
O(1)−Co(1)−O(2)	152.0(1)	150.11(5)
O(1)−Co(1)−O(11)	94.0(1)	94.55(5)
O(1)−Co(1)−O(12)	93.7(1)	96.86(5)
O(2)−Co(1)−O(11)	93.32(9)	85.53(5)
O(2)−Co(1)−O(12)	93.0(1)	97.15(5)
O(11)−Co(1)−O(12)	152.9(1)	151.30(5)
O(1)−C(6)−O(3)	126.7(4)	125.4(2)
O(2)−C(7)−O(4)	125.6(3)	125.8(2)
O(12)−C(17)−O(14)	125.5(3)	126.7(2)
O(11)−C(16)−O(13)	125.8(3)	125.6(2)
Co(1)−N(1)−C(1)	118.3(3)	120.5(1)
Co(1)−N(1)−C(5)	120.7(2)	118.2(1)
Co(1)−N(11)−C(11)	120.4(2)	120.2(1)
Co(1)−N(11)−C(15)	118.8(2)	119.5(1)
Co(1)−O(1)−C(6)	116.1(3)	115.5(1)
Co(1)−O(2)−C(7)	113.3(2)	115.4(1)
Co(1)−O(11)−C(16)	114.4(2)	115.5(1)
Co(1)−O(12)−C(17)	116.2(2)	113.6(1)
O(14)−Co(2)−O(21)		95.65(5)
O(14)−Co(2)−O(22)		90.48(5)
O(14)−Co(2)−O(23)		80.07(6)
O(14)−Co(2)−O(25)		170.46(5)
O(14)−Co(2)−O(24)		79.84(5)
O(21)−Co(2)−O(22)		89.39(6)
O(21)−Co(2)−O(23)		176.62(6)
O(21)−Co(2)−O(25)		85.63(5)
O(21)−Co(2)−O(24)		85.96(6)
O(22)−Co(2)−O(23)		88.5(5)
O(22)−Co(2)−O(24)		168.79(6)
O(22)−Co(2)−O(25)		98.99(6)
O(23)−Co(2)−O(24)		96.58(7)
O(23)−Co(2)−O(25)		92.09(6)
O(24)−Co(2)−O(25)		90.86(6)

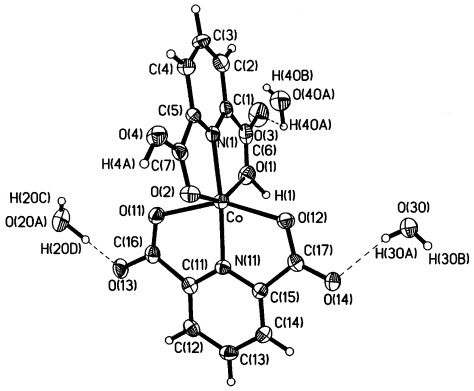

Figure 2. Molecular structure and atomic labeling scheme for complex [Co(II)(H_2dipic)(dipic)]·3H_2O (**3**), with ellipsoids drawn at the 50% probability level. The water molecule (containing O20, H20A, and H20B) is shown in a symmetry-related position and numbered O20A, H20C, and H20D (see also Table 3).

complex ([Ag(Hdipic)$_2$]·H_2O)[24] and a copper(II) complex ([Cu(Hdipic)$_2$]·3H_2O).[23]

Different coordination modes have been reported in transition metal−dipicolinate complexes. The coordination modes observed in the solid state as well as two new coordination modes introduced in this work (b and d) are summarized in Figure 1. The most common coordination mode is a in which the metal is coordinated to the long C−O bond. This coordination mode is found in [Ni(Hdipic)$_2$]·3H_2O,[15−17] [Zn(Hdipic)$_2$]·3H_2O,[18,19] [Zn$_2$(dipic)$_2$]·7H_2O,[18] [Fe(Hdipic)$_2$(OH_2)],[20] [Fe$_2$(dipic)$_2$(OH_2)$_6$]·2H_2dipic,[20] [Fe$_3$(dipic)$_2$(Hdipic)$_2$(H_2O)$_4$]·2H_2O,[21] [Fe$_2$(dipic)$_2$(H_2O)$_5$]·2.25H_2O,[21] [Fe$_3$(dipic)$_4$(H_2O)$_6$(NH_4)$_2$]·4H_2O·2H_2dipic,[21] [Fe$_{13}$(Hdipic)$_6$(dipic)$_{10}$(H_2O)$_{24}$]·13H_2O,[21] [Cu(dipic)(H_2O)$_2$],[22] and [Cu(H_2dipic)(dipic)]·H_2O.[19] Another common coordination mode found in complexes with monoprotonated Hdipic is represented by c and found in [Ni(Hdipic)$_2$]·3H_2O,[15−17] [Zn(Hdipic)$_2$]·3H_2O,[18,19] [Fe(Hdipic)$_2$(OH_2)],[20] [Fe$_3$(dipic)$_2$(Hdipic)$_2$(H_2O)$_4$]·2H_2O,[21] [Fe$_{13}$(Hdipic)$_6$(dipic)$_{10}$ (H_2O)$_{24}$]·13H_2O,[21] and [Cu(H_2dipic)(dipic)]·H_2O.[19,23] A coordination mode in which the C−O bonds are of equal length is e, which has been observed in [Ag(Hdipic)$_2$]·H_2O,[24] [Cu(H_2dipic)(dipic)]·3H_2O,[19,23] and [Zn(Hdipic)$_2$]·3H_2O.[19] Less commonly observed coordination modes involve coordination of two metal ions to one carboxylate group and are represented by f (observed in [Fe$_3$(dipic)$_2$(Hdipic)$_2$(H_2O)$_4$]·2H_2O,[21] [Fe$_2$(dipic)$_2$(H_2O)$_5$]·2.25H_2O,[21] and [Fe$_{13}$(Hdipic)$_6$(dipic)$_{10}$(H_2O)$_{24}$]·13H_2O),[21] g (observed in [Zn$_2$(dipic)$_2$]·7H_2O),[18] and h (observed in [Fe$_2$(dipic)$_2$(OH_2)$_6$]·2H_2dipic).[20] The key differences in the two new coordination modes are the coordination of the metal ion to the short C═O bond (in b) and to the oxygen atom carrying the proton (in d).

The formula unit contains 3 water molecules, 1 of which is disordered in the crystal structure (O(40)). The other 2 water molecules form hydrogen bonds with the dianionic dipic ligand**.** Additional hydrogen bonding between water molecules O(20) and O(40) was found (Table 3). The major component of O40 (i.e., O40A) is well defined, and hydrogen bonding distances are O(30)···H(4A) (1.54(5) Å), O(20)···H1 (1.51(5) Å), O(13)···H(20B) (1.48(5) Å), O(14)···H(30A) (1.98(5) Å), and O(14)···H(30B) (1.95(5) Å). Hydrogen bonds are formed between a H-donor and a H-acceptor, and those hydrogen bonds in which the proton originates in [Co(II)(H_2dipic)(dipic)] are shorter than those in which [Co(II)(H_2dipic)(dipic)] is the H-acceptor. An exception to this pattern is observed when the H-acceptor is a carboxylate group bound in coordination mode b. The two H_2O molecules (O(30) and O(20)) link two complexes through hydrogen bonds. The relevant distances are 1.98(5) Å (H(30A)···O(14)), 1.54(5) Å (O(30)···H(4A)), 1.48(5) Å (H(20B)···O(13)) and 1.51(5) Å (O(20)···H(1)). As mentioned in the Experimental Section, all hydrogen atoms except those of the disordered water oxygen atom O40 were found in the electron density map at the expected orientation. The O−H bond lengths are, however, relatively imprecise as indicated by the tabulated errors.

Table 3. Hydrogen Bonds for [Co(II)(H_2Dipic)(dipic)]·3H_2O (**3**)

D−H···A	*d*(D−H)	*d*(H···A)	*d*(D···A)	∠(DHA)
O(20)−H(20A)···O(40A)	0.68(5)	1.94(5)	2.572(11)	157(7)
O(30)−H(30A)···O(14)	0.73(5)	1.98(5)	2.690(4)	165(5)
O(1)−H(1)···O(20) #1[a]	1.09(5)	1.51(5)	2.595(4)	177(4)
O(4)−H(4A)···O(30) #2	0.95(5)	1.54(5)	2.469(4)	166(5)
O(20)−H(20B)···O(13) #3	0.99(5)	1.48(5)	2.465(4)	174(5)
O(30)−H(30B)···O(14) #4	0.82(5)	1.95(5)	2.730(4)	159(5)

[a] Symmetry transformations used to generate equivalent atoms: #1 $-x+1, -y, -z+1$; #2 $x, -y+3/2, z+1/2$; #3 $-x+1, y-1/2, -z+3/2$; #4 $-x+2, -y+1, -z+1$.

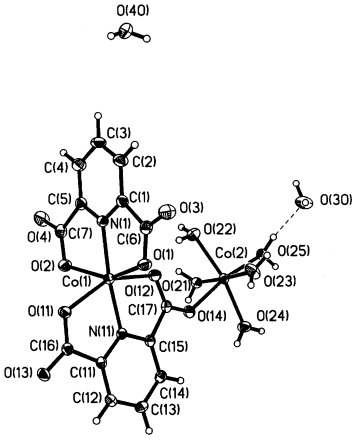

Figure 3. Molecular structure and atomic labeling scheme for complex [Co(II)(dipic)(μ-dipic)Co(II)(H_2O)$_5$]·2H_2O (**4**), with ellipsoids drawn at the 50% probability level.

Crystal Structure of [Co(II)(dipic)(μ-dipic)Co(II)(H_2O)$_5$]·2H_2O (4). The crystal data are shown in Table 1. The molecular structure is depicted in Figure 3. The two dipic ligands are deprotonated in the complex. Both dipic^{2-} ligands are coordinated in a tridentate manner to one cobalt atom; one of the two dipic^{2-} groups also acts as a bridging ligand to the pentaaquo−Co(II) unit. This type of complex has previously been observed in [Zn$_2$(H_2O)$_5$(dipic)$_2$]·2H_2O.[18] Both of the two Co(II) ions exhibit distorted octahedral geometry. The Co−N bond distances are 2.026(2) and 2.033(1) Å, and the Co(1)−O bond distances range from 2.123(1) to 2.225(1) Å (average 2.182 Å). The carboxylate groups are bound in coordination modes a and f. The Co(2) atom is bound to six oxygen atoms, one from the carboxylate (Co(2)−O(14) 2.097(1) Å) and the other five from water

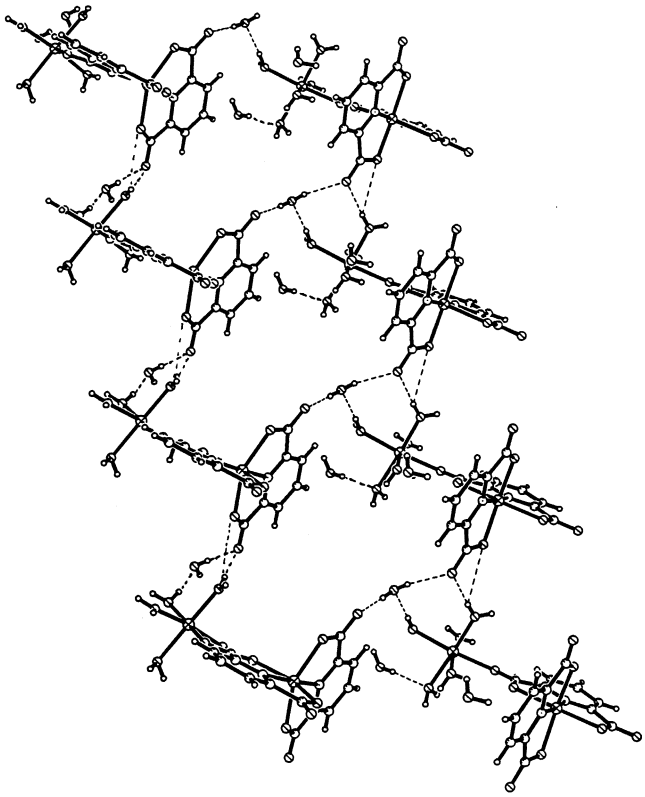

Figure 4. Crystal packing diagram of [Co(II)(dipic)(μ-dipic)Co(II)-$(H_2O)_5$]·$2H_2O$.

molecules (Co−O from 2.060(2) to 2.180(1) Å, average Co(2)−O 2.097 Å for coordinated water).

Strong hydrogen bonding exists in the crystal structure (Figure 4). Hydrogen bonding between coordinated water (O(23)) and the carboxylate oxygen atoms (O(2) and O(4)) of the dipic^{2-} links the binuclear cobalt molecules to form a one-dimensional chain. The water molecule (O(30)) which hydrogen bonded to three complex molecules stabilizes the chain structure. Relevant distances are 1.81(3) Å (H(25B)···O(30)), 1.95(3) Å (H(30A)···O(3)), 2.08(3) Å (H(30B)···O(4)), 1.92(3) Å (H(23A)···O(4)), 2.10(3) Å (H(40B)···O(21)) and others listed in Table 4. Hydrogen bonds are indicated in Figure 3 with dashed lines. The hydrogen bonds in this structure do not appear to be as strong as those in [Co(II)(H_2dipic)(dipic)]·$3H_2O$.

IR Spectroscopy. The IR spectra of the 1:2 and 2:2 Co(II) complexes are similar. The vibrations of $\nu_{as}(CO_2^-)$ and $\nu_s(CO_2^-)$ are very strong at 1620−1640 cm^{-1} and 1370−1390 cm^{-1}. The OH vibration of water is a strong and dominating broad peak at 3200−3600 cm^{-1} in IR spectra. In the [Co(Hdipic)$_2$] complex, a shoulder peak around 1700 cm^{-1} is attributed to the protonated carboxylate in the complex, and the $\nu_s(CO_2^-)$ contains three peaks, 1396, 1381, 1367 cm^{-1}, which may be related to the hydrogen bonding system. In the Co(III) complex, the $\nu_{as}(CO_2^-)$ are found at higher frequencies with two peaks at 1664 and 1649 cm^{-1}, and the $\nu_s(CO_2^-)$, at lower frequency (1333 cm^{-1}) than in the Co(II) complexes.

A correlation of the carboxylate coordination mode to metal ions was made by examining the difference between

Table 4. Hydrogen Bonds for [Co(II)(dipic)(μ-dipic)Co(II)$(H_2O)_5$]·$2H_2O$ (**4**)

D−H···A	*d*(D−H)	*d*(H···A)	*d*(D···A)	∠(DHA)
O(22)−H(22A)···O(12)	0.82(3)	2.07(3)	2.8328(19)	155(2)
O(25)−H(25B)···O(30)	0.86(3)	1.81(3)	2.662(2)	170(3)
O(21)−H(21A)···O(13) #1[a]	0.76(3)	1.93(3)	2.689(2)	173(3)
O(21)−H(21B)···O(1) #2	0.85(3)	1.96(3)	2.8006(18)	172(2)
O(22)−H(22B)···O(3) #2	0.81(3)	1.91(3)	2.7090(19)	171(3)
O(23)−H(23A)···O(4) #3	0.81(3)	1.92(3)	2.727(2)	177(3)
O(23)−H(23B)···O(40) #4	0.78(3)	2.09(3)	2.830(2)	158(3)
O(24)−H(24A)···O(13) #5	0.88(3)	1.77(3)	2.6472(18)	176(3)
O(24)−H(24B)···O(40) #6	0.73(3)	2.27(3)	2.970(2)	161(3)
O(25)−H(25A)···O(11) #5	0.82(3)	1.96(3)	2.7745(18)	172(2)
O(30)−H(30A)···O(3) #7	0.84(3)	1.95(3)	2.783(2)	176(3)
O(30)−H(30B)···O(4) #3	0.73(3)	2.08(3)	2.787(2)	163(3)
O(40)−H(40A)···O(2) #4	0.79(2)	2.34(2)	3.0394(19)	148(2)
O(40)−H(40A)···O(11) #4	0.79(2)	2.58(2)	3.213(2)	139(2)
O(40)−H(40B)···O(21) #8	0.83(2)	2.10(3)	2.9174(19)	168(2)

[a] Symmetry transformations used to generate equivalent atoms: #1 $-x+1, -y, -z+3$; #2 $x-1, y, z$; #3 $x, y, z-1$; #4 $x, -y+1/2, z-1/2$; #5 $x-1, y, z-1$; #6 $-x+1, y-1/2, -z+5/2$; #7 $x-1, -y+1/2, z-1/2$; #8 $x+1, -y+1/2, z+1/2$.

ν_{as} and ν_s of the complexes.[37] These studies were demonstrated with series of complexes from acetate and other carboxylic acids; however, none of these complexes included dipicolinic acid. Regardless, examining whether the values for acetate complexes determined previously would serve as a model system for the complexes described in this paper, the $\nu_{as}-\nu_s$ values and the prediction of their binding mode was checked. The difference amounted to values between 200 and 350 cm^{-1}, which is consistent with unidentate coordination modes. Thus, although a variety of different coordination modes are observed in these complexes, the coordination modes are unidentate as predicted. This observation suggests that this difference in $\nu_{as}-\nu_s$ could be used as indicative of coordination modes observed in these types of complexes.

The light purple solid (from preparation) has a different IR spectrum from those of 1:2 or 2:2 species, and the NMR spectra suggest the existence of a 1:1 Co(II) species. The $\nu_{as}(CO_2^-)$ is at 1686 and 1639 cm^{-1}, and the former peak is more intense. The $\nu_s(CO_2^-)$ is of medium intensity with three peaks at 1330, 1289, and 1257 cm^{-1}. No free ligand was observed in the NMR spectra or the IR spectra indicating that all ligand present is coordinated to the cobalt. Furthermore, the NMR spectra show no line broadening indicative of dynamic processes involving free ligand. These results and the elemental analysis are consistent with this purple solid also containing free $CoCl_2$ (up to 20%).

Solution Characterization. Structure and Stability of Complexes as Monitored by NMR Spectroscopy. ^{1}H NMR spectra were recorded for both Co(II) and Co(III) dipic complexes. The solution chemistry of these complexes will be described here. Figure 5 shows the spectra of the solutions prepared from crystals of the four pure solid Co(II)−dipic complexes. Each of these compounds produces solutions for which paramagnetic NMR spectra of high spin compounds were obtained.

(37) Nakamoto, K. *Infrared and Raman Spectra of Inorganic and Coordination Compounds*, 5th ed.; John Wiley & Sons: New York, 1997; Part B, pp 58−63.

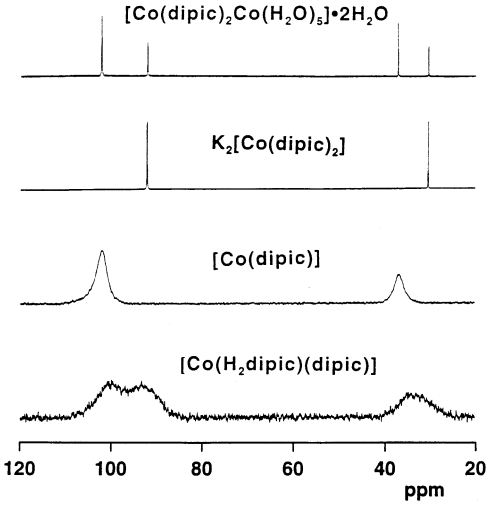

Figure 5. ^{1}H NMR spectra of Co(II)−dipic complexes [Co(II)(H_2dipic)(dipic)]·3H_2O (9.0 mM, pH 1.8), Co(II)(dipic)·3.5H_2O (28 mM, pH 1.6), K_2[Co(II)(dipic)$_2$]·7H_2O (10 mM, pH 7.3), and [Co(II)(dipic)(μ-dipic)Co(II)(H_2O)$_5$]·2H_2O (14 mM, pH 6.4).

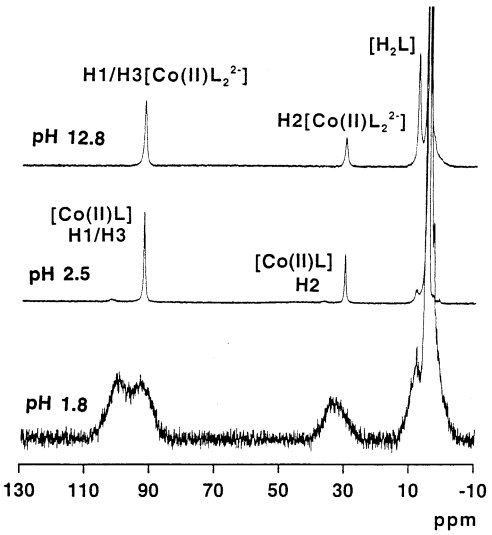

Figure 6. ^{1}H NMR spectra of 9.0 mM [Co(II)(H_2dipic)(dipic)]·3H_2O dissolved in deuterium oxide at pH 1.8, 2.5, and 12.8.

[Co(II)(H_2dipic)(dipic)]·3H_2O. Crystals of [Co(II)(H_2dipic)(dipic)]·3H_2O were dissolved in deuterium oxide solution resulting in a solution of pH 1.8 (Figures 5 and 6). A set of broad peaks was observed at high magnetic field, and two broader peaks were observed at lower magnetic field. Spiking experiments indicated that a signal overlapping with the HOD signal arose from free ligand in Figure 5 (data not shown). In Figure 6, the ^{1}H NMR spectra are shown of deuterium oxide solutions containing 9.0 mM [Co(II)(H_2dipic)(dipic)]·3H_2O at three pH values. In these spectra, the free ligand signal is observed at 8 ppm at low pH. Increasing the pH above 2 leads to spectra with two sharp signals. Thus, the broad doublet (1:1) changes into one sharp singlet with a minor signal (<5%) at lower field. This spectrum is consistent with the interpretation that at pH 2.1 one major species exists in solution, whereas at pH 1.8 two complexes exist in equal amounts (see a following paragraph for substantiation of this interpretation). As the pH is increased above pH 3, the minor signal is no longer observable. In

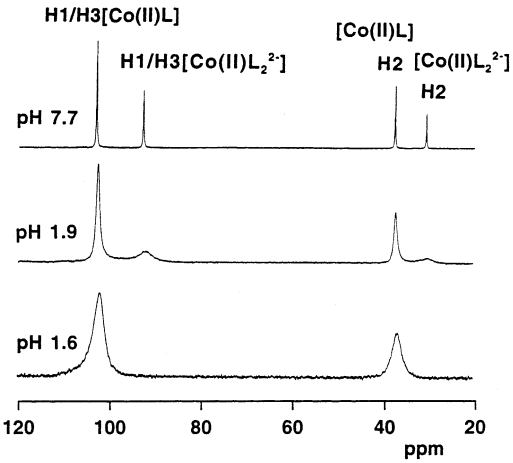

Figure 7. ^{1}H NMR spectra of 28 mM Co(II)(dipic)·3.5H_2O dissolved in deuterium oxide at pH 1.6, 1.9, and 7.7.

Figure 6, we show a spectrum at pH 12.8 to document the stability of the complex; however, above this pH, the complex begins to hydrolyze and forms free ligand. Studies described later with [Co(II)(dipic)$_2$]$^{2-}$ will show that the major species formed in the pH range 2.5−12.8 is the 1:2 complex. Studies shown later with solid Co(II)(dipic)·3.5H_2O suggest that the minor species is the 1:1 complex.

[Co(II)(dipic)$_2$]$^{2-}$. The grayish-brown crystalline solid of [Co(II)(dipic)$_2$]$^{2-}$ gives light brown solutions from which ^{1}H NMR spectra with only two signals are obtained (Figure 5). The signals at 30.6 (H2) and 92.6 (H1/H3) ppm give coordination-induced shifts (CIS) of 22.5 and 84.5 ppm at 20 °C and pH 5.1, respectively. ^{1}H NMR spectra of a deuterium oxide solution containing [Co(II)(dipic)$_2$]$^{2-}$ in the presence of excess free ligand from pH 1.3 to 12.3 were recorded (data not shown). Because the two signals at 30.6 and 92.6 ppm remain unchanged and a signal from the free ligand signal appears, we conclude that the complex observed at 92.6 and 30.6 ppm is the 1:2 complex.

Co(II)(dipic)·3.5H_2O. Solid Co(II)(dipic)·3.5H_2O was dissolved in deuterium oxide solution giving a solution of pH 1.6. The two ^{1}H NMR signals (36 ppm for H2, 101 ppm for H1/H3) were broad (Figure 7); however, the chemical shifts were at the same positions observed for the major complex shown for [Co(dipic)(μ-dipic)Co(H_2O)$_5$]·2H_2O in Figure 5. Raising the pH value of the solution decreased the line width of the NMR signals, and signals relating to a 1:2 species appeared. At pH 7.7, the proportions of the 1:1 and 1:2 complexes are 65% and 35%, respectively. No peaks attributable to the free ligand were observed; however, on the basis of the 1:1 stoichiometry of the solid added to the solution, an additional 35% of free Co^{2+} formed. On the bais of these spectra, we conclude that the 1:1 complex does form in aqueous solution at low concentrations and in the pH region from 2 to 7. NMR signals for this 1:1 species were also observed by adding solid $CoCl_2$ to the deuterium oxide solution of [Co(II)(dipic)$_2$]$^{2-}$.

[Co(II)(dipic)(μ-dipic)Co(II)(H_2O)$_5$]·2H_2O. Four ^{1}H NMR signals were observed (30.5, 37.3, 92.3, 102.5, ppm, pH 6.4, 18 °C) for the deuterium oxide solution from crystals of [Co(II)(dipic)(μ-dipic)Co(II)(H_2O)$_5$]·2H_2O. Spiking experi-

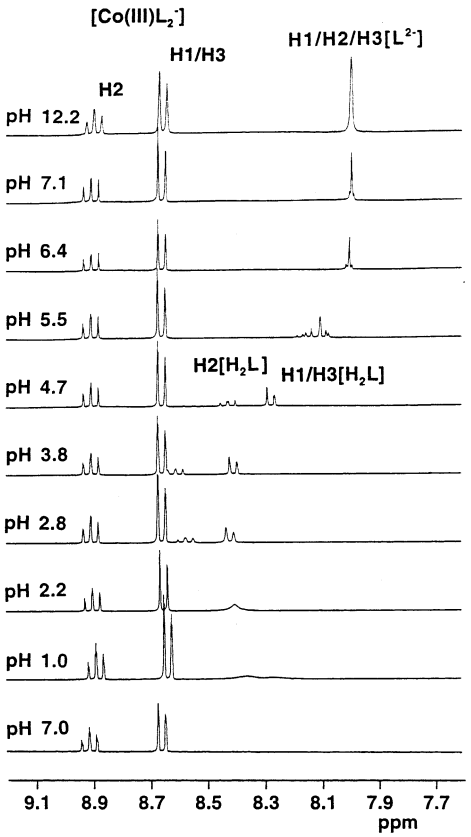

Figure 8. ^{1}H NMR spectra of 2.7 mM K[Co(III)(dipic)$_2$] dissolved in deuterium oxide at pH 7.0 (bottom). The additional spectra shown are of solutions containing 28 mM [Co(III)(dipic)$_2$]$^-$ in the presence of 47 mM H_2dipic. These spectra are shown from pH 1 to pH 12.2.

ments with the free ligand and [Co(II)(dipic)$_2$]$^{2-}$ let us assign the signals at 30.5 and 92.3 ppm to the [Co(II)(dipic)$_2$]$^{2-}$ complex. In analogy with studies described previously, the signals at 37.3 and 102.5 ppm are attributed to the 1:1 species. On the basis of these NMR spectra, it is clear that this complex is unstable in aqueous solution and forms both 1:1 (64%) and 1:2 (36%) species. The conversion of [Co(dipic)(μ-dipic)Co(H_2O)$_5$]·2H_2O to [Co(dipic)(H_2O)$_3$] and [Co(dipic)$_2$]$^{2-}$ does take place in solution on the NMR time scale. Furthermore, the lack of signal for the free ligand further demonstrates the high stability of the 1:2 and 1:1 complexes.

[Co(III)(dipic)$_2$]$^-$. The [Co(III)(dipic)$_2$]$^-$ complex gives a ^{1}H NMR spectrum expected for a low spin diamagnetic compound with two signals at 8.65 (H1/H3) and 8.90 (H2) ppm (CIS of 0.57 and 0.75 ppm, 20 °C, pH 5.5). These shifts are consistent with that expected for a complex containing a tridentate ligand. Figure 8 shows the spectra of solid K[Co(III)(dipic)$_2$] dissolved in deuterium oxide solution at pH 7.0. In addition, we show the spectra of [Co(III)(dipic)$_2$]$^-$ in the presence of excess ligand at various pH values. Although the signals for the H_2dipic/Hdipic$^-$/dipic^{2-} vary significantly, no change is observed for the complex as a function of pH. The invariance of the complex ^{1}H NMR signals was also recently observed for [VO_2dipic]$^-$.[5]

The spectra in Figure 8 document the high stability of the [Co(III)(dipic)$_2$]$^-$ anion. From pH 1 to 12, a large fraction of the [Co(III)(dipic)$_2$]$^-$ complex remains intact. However, as the solution becomes increasingly alkaline, increasing amounts of the complex hydrolyze to give increasing concentrations of free ligand. Solutions of solid K[Co(III)(dipic)$_2$] (in the absence of excess dipic^{2-}) confirm this interpretation by showing no evidence for free ligand below pH 8.2. The stability of this complex is superior to that of, for example, [VO_2dipic]$^-$ that begins to dissociate at pH 7.[5]

^{13}C NMR Spectra. ^{13}C NMR spectra were recorded to confirm the observations described previously. Using routine parameters to record the coupled ^{13}C NMR spectrum of [Co(II)(dipic)$_2$]$^{2-}$, a spectrum was observed with six signals at −128.9, −152.6, 361.3, 363.5, 370.4, and 372.3 ppm (22.0 °C). Because the signals are observed in a large window, additional decoupling experiments were necessary to assign the signals. When selecting at 91 ppm (25916 Hz), the four signals (two doublets) collapsed to one signal at 359.4 ppm and a broad signal at 370 ppm, showing that the protons (H1/H3) at 91 ppm are responsible for the splitting. Selecting at 28.3 ppm (6961 Hz) changed the two doublets of doublets to a signal at 368.9 ppm and a broad signal at 360.1 ppm. These spectra support the assignment of the signal at 359.4 ppm to C3 and the signal at 360.1 ppm to C2/C4. The two signals at high field are attributed to the ipso carbons (C1/C5) and the two carboxylates. The chemical shifts for the [Co(III)(dipic)$_2$]$^-$ are 132.3, 146.6, 155.4, and 175.2 ppm. Given the chemical shifts for free ligand (130.4, 138.3, 148.6, and 167.4 ppm), the ^{13}C NMR data support the conclusion that the ligand is coordinated in a tridentate manner to the Co atom. Unfortunately, the limited solubility of the complexes at acidic pH prevented the acquisition of 2D ^{13}C NMR spectra of the Co(II) and Co(III) dipic complexes.

Absorption Spectroscopy of Complexes. The complex colors indicate the existence of absorbance bands in the visible region. Both the ligand and complex absorb strongly in the UV−visible spectral region up to about 350 nm, but at higher wavelengths, only the complex absorbs. The K[Co(dipic)$_2$] complex has one absorption maximum at about 511 nm. This is a d−d transition consistent with other reported d−d transitions at about 500 nm in *cis*-[Coen$_2$F$_2$]$^+$ (low spin).[38] This maximum persists from pH 0.7 to pH 12.1 and has an extinction coefficient of 670 cm^{-1} M^{-1}. A shoulder at about 350−400 nm is also observed in contrast to K_2[Co(dipic)$_2$] where a higher absorption band is observed up until about 420 nm. The K_2[Co(dipic)$_2$] complex has more absorption maxima with the major two at 460 and 583 nm. These signals are assigned to d−d transitions analogous with the d−d transitions observed in, for example, [Co(H_2O)$_6$]$^{2+}$ at about 530 nm.[38] The extinction coefficients of these complexes are about 30-fold less than the Co(III) complex at 16 and 17 cm^{-1} M^{-1}. In addition, a small shoulder at about 530 nm is observed; this peak is distinct from that observed in the Co(III)−dipic complexes. In solutions of the Co(II) complex, oxidation to the Co(III) complex can readily be observed by the signal at 510 nm between the two absorption bands. The absorption spectra show that the bands at 460,

(38) Cotton, F. A.; Wilkinson, G. *Advanced Inorganic Chemistry*, 4th Ed.; John Wiley & Sons: New York, 1980; pp 772−775.

510, and 583 nm are diagnostic for these complexes. Furthermore, the absorption spectroscopy confirmed the high stability of the complexes observed by NMR spectroscopy.

Variable Temperature and ^{1}H EXSY NMR Spectroscopy of Co(II) and Co(III) Complexes. The VT-^{1}H NMR spectra and ^{1}H EXSY NMR spectra were recorded for three different types of samples to examine whether various types of exchange reactions took place. In samples containing $[Co(III)(dipic)_2]^-$ and excess free ligand H_2dipic at pH 6.4, no evidence for exchange between complex and free ligand was observed. To confirm the lack of ligand exchange in this system, ^{1}H EXSY NMR spectra were run on solutions from pH 1.0 to 12.3.

In samples containing both $[Co(III)(dipic)_2]^-$ and $[Co(II)(dipic)_2]^{2-}$ at pH 7.0, the possibility of the exchange of ligands between Co(II) and Co(III) complexes was investigated. The signals for both the $[Co(III)(dipic)_2]^-$ and $[Co(II)(dipic)_2]^{2-}$ complexes broadened slightly and moved toward each other upon increasing the temperature from 32 to 70 °C. However, the broadening and shifts of the signals are small, consistent with the expectation that exchange or electron-transfer processes are very slow. The five different EXSY spectra that were recorded for samples of $[Co(III)(dipic)_2]^-$ and $[Co(II)(dipic)_2]^{2-}$ complexes from pH 1.7 to pH 7.2 did not show any observable cross-signals indicative of interchange.

Variable temperature ^{1}H NMR spectra were recorded of a deuterium oxide solution of crystalline [Co(II)(dipic)-(μ-dipic)Co(II)$(H_2O)_5$]·$2H_2O$ which, as described previously, forms a solution that contains $[Co(II)(dipic)_2]^{2-}$ and Co(II)-(dipic) at pH 6.4. The signals broadened, and the separation between the H1/H3 protons in the 1:1 and 1:2 species decreased while overall the signals moved to higher field with increasing temperature. This pattern is consistent with slow exchange on the time scale of the ^{1}H NMR experiment. The ^{1}H EXSY NMR spectra were recorded on a sample with a total concentration of 13.9 mM Co(II) at pH 6.4. Given in Figure 9 is an excerpt of the spectrum specifically showing the exchange between H2 in the 1:1 and 1:2 complexes. Conversion between the 1:1 and 1:2 complexes on the NMR time scale is thus confirmed in these experiments.

Exchange Reaction of $[Co(II)(dipic)_2]^{2-}$ as a Function of pH. To further explore the reactivity of $[Co(II)(dipic)_2]^{2-}$, ^{1}H EXSY NMR spectra were recorded of this species in the presence of free ligand H_2dipic over the pH range 1.3−12.3. Because Co(II) is d^7, the complex contains at least one unpaired electron, and the EXSY NMR spectra must be recorded over a wide chemical shift window with paramagnetic parameters. The unpaired electron broadens and shifts the ^{1}H NMR signals so that scalar coupling information is lost in these spectra. Previously, 2D ^{1}H NMR spectra have been recorded for several paramagnetic Co(II) complexes, documenting the validity of the chemical shift and intensity information in these measurements.[39,40]

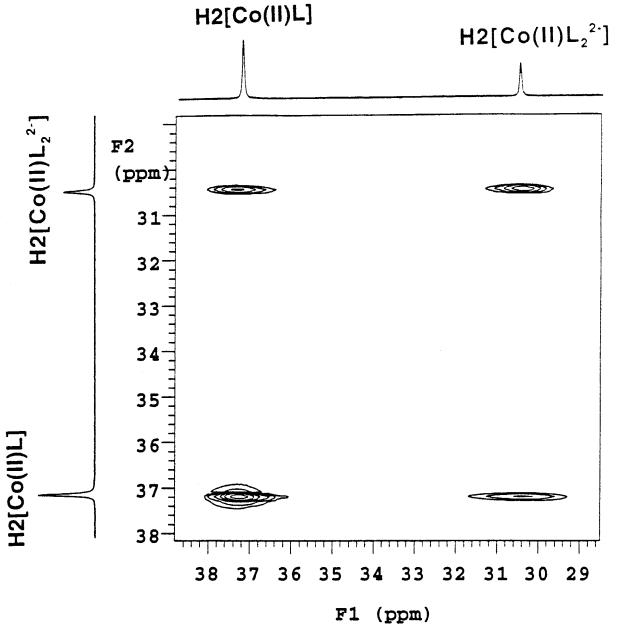

Figure 9. Partial ^{1}H EXSY spectrum of the solution containing 13.9 mM [Co(II)(dipic)(μ-dipic)Co(II)$(H_2O)_5$]·$2H_2O$ at pH 6.4; the solution contains 8.8 mM [Co(II)dipic] and 5.1 mM $[Co(II)(dipic)_2]^{2-}$. The mixing and delay times used are 0.10 and 0.30 s, respectively.

^{1}H NMR EXSY spectra were recorded at pH 3.3, 4.1, 5.1, 7.2, 7.8, 9.9, and 12.3, and two representative spectra are shown in Figure 10. The observation of cross-peaks between the complex and the free ligand for both protons confirms the ligand−complex exchange (Figure 10). Exchange was observed at all pH values as cross-peaks between the (H1/H3)/H2 of the complex and the (H1/H3)/H2 of the ligand. The chemical shifts for the free ligand and complex varied with pH, and accordingly, on the basis of chemical shift differences, some changes in cross-signal intensities would be anticipated. However, the cross-peak volume intensity changes to a greater extent than would be justified on the basis of the differences in chemical shifts as a function of pH. As the pH approaches 5, the cross-peak volumes decrease significantly. But as the pH is increased above 9.9, the volume of the cross-peaks increases, corresponding to a more rapid ligand exchange. In Figure 11, the exchange volume intensities (the exchange between H2 in the $[Co(II)(dipic)_2]^{2-}$ and free ligand) are shown expressed as the ratio of total complex to ligand exchange volume integral over the corresponding diagonal signal as a function of pH. As shown in Figure 11, the exchange is slowest from pH 5 to 10. We conclude that the complex is the least labile in the pH region 5−10. The exchange of free ligand in this complex is reminiscent of the pH dependent exchange observed in the $[VO_2dipic]^-$ complex reported previously.[5]

The ^{1}H EXSY NMR spectra at different pH also show an important difference. One dominant cross-peak observed in spectra of solutions with pH values below 4 or above 12 is of significantly lower intensity from pH 5 to 10 for $[Co(II)(dipic)_2]^{2-}$. In Figure 10 (a), this cross-peak is indicated using dotted lines. This cross-peak is indicative of scalar coupling at pH 5−10, and a similar signal was observed for the related $[VO_2dipic]^-$ complex.[5] However,

(39) Cotton, F. A.; Murillo, C. A.; Wang, X. *Inorg. Chem.* **1999**, *38*, 6294−6297.
(40) Epperson, J. D.; Ming, L.-J.; Woosley, B. D.; Baker, G. R.; Newkome, G. R. *Inorg. Chem.* **1999**, *38*, 4498−4502.

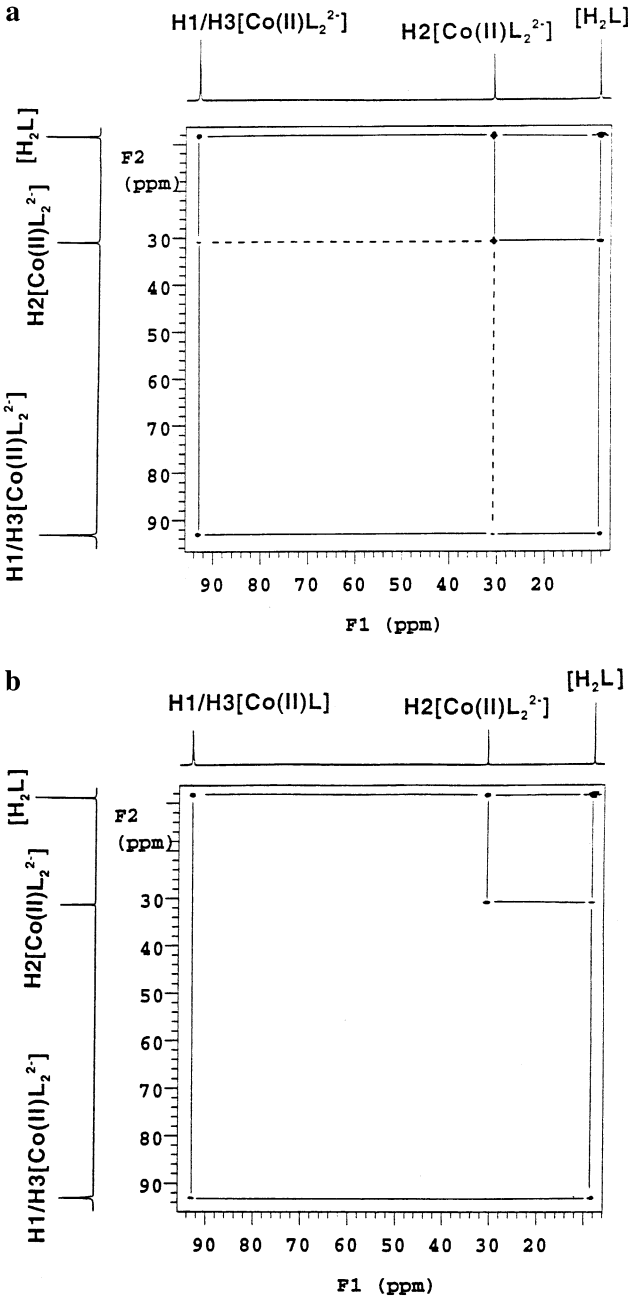

Figure 10. Two representative ^{1}H EXSY spectra of a solution containing 28 mM $[Co(II)(dipic)_2]^{2-}$ and 27 mM H_2dipic at pH 3.3 (a) and 4.1 (b). The solid lines connect the observed cross-peaks. Dotted lines are due to scalar coupling and are only observed in the spectrum at pH 3.3. The mixing and delay times used are 0.12 and 0.05 s, respectively.

at pH below 4 and above 10, this signal is much more intense, reflecting the superimposed cross-peak due to exchange. The pH dependent ligand−complex exchange is presumably associated with the differences in the protonation states of the complex and/or ligand. The rate of complex formation is a result of the combined presence of Co(II) complexes and the nucleophilicity of the ligand, whether it be $dipic^{2-}$, $Hdipic^-$, H_2dipic, or H_3dipic^+.[3] The small observed change in the chemical shift as the pH is decreased is attributed to species $[Co(dipic)(Hdipic)]^-$ and $[Co(dipic)_2]^{2-}$ coexisting in aqueous solution below pH 4. Therefore, as the solution becomes acidic, the protonation of $[Co(II)(dipic)_2]^{2-}$ gives $[Co(dipic)(Hdipic)]^-$ and $[Co(Hdipic)]^+$ which are expected to be more readily attached than $[Co(II)(dipic)_2]^{2-}$ by the ligand nucleophiles.

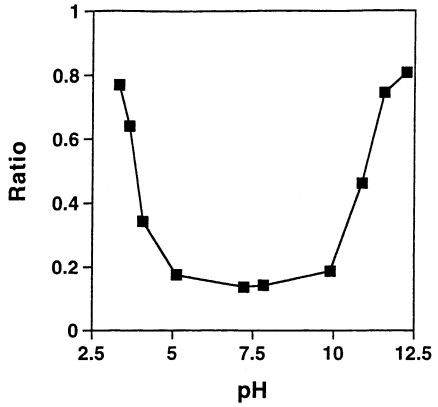

Figure 11. Ratio of total volume integrals of exchange cross-signals (H2) between $[Co(II)(dipic)_2]^{2-}$ and free ligand and the total volume integrals of the diagonal signals (H2) obtained from ^{1}H EXSY NMR spectra plotted as a function of pH.

Rationale for Selection of Cobalt Compound for Animal Studies. The chemical studies described here presented several possible cobalt complexes to be considered for administration to STZ-induced diabetic rats. We have previously shown that the $NH_4[VO_2dipic]$ has insulin-like activity despite its properties (this compound is not stable at neutral pH; the complex is an anion and is also labile).[5] Although both the Co(II) and Co(III) compounds are significantly more stable than their vanadium counterparts, the Co(II) complex is labile, as is $[VO_2dipic]^-$. Furthermore, a Co(II)−dipicolinate complex is most compatible with the reducing cellular environment.[4] $K_2[Co(dipic)_2]$ was therefore considered to be the best compound to initially test the insulin-like activity of organic cobalt complexes.

Insulin-Like Effects of $K_2[Co(dipic)_2]$ in Rats with STZ-Induced Diabetes. The effect of $[Co(dipic)_2]^{2-}$ on reducing the hyperglycemia of diabetes was tested using normal and untreated diabetic animals as controls. $VOSO_4$ treatment, frequently used to lower diabetic hyperglycemia in rats, was used as a positive control for metal efficacy in alleviating symptoms of diabetes. In contrast to $VOSO_4$, $[Co(dipic)_2]^{2-}$ was found to have a very limited effect in lowering diabetic hyperglycemia, showing only statistically significant ($p \leq 0.05$ vs diabetic) lowering of blood glucose for 1 day out of 5 days tested in a 2 week period (data not shown). Over this 2 week treatment period, the $[Co(dipic)_2]^{2-}$ treated animals ingested 0.96 + 0.01 mmol/Co/Kg per day, while the $VOSO_4$ treated animals ingested 0.49 + 0.02 mmol V/klg per day. In this experiment, the weight after 2 weeks for the cobalt treated animals (227 ± 4 g) was less than that of the normal animals (337 ± 11 g) but similar to that of the untreated diabetic animals (246 ± 6 g). These weights for the diabetic and cobalt treated diabetic rats were not statistically significant in our ANOVA analysis. The $VOSO_4$ treated animals, after an initial loss of weight, maintained their weight throughout the experiment (180 ± 11 g) which at the end of 2 weeks was statistically significantly lower ($p \leq 0.001$) compared to that of the diabetic animals. Reduction in body

Table 5. Effects of 4 Weeks of Treatment of $K_2[Co(dipic)_2]$ and $VOSO_4$ on the Serum Lipid Levels of Wistar Rats with STZ-Induced Diabetes Were Determined[a]

group/treatment	*n*	triglyceride (mg/dl)	cholesterol (mg/dl)	final weight (g)	final blood glucose level (mg/dl)	fluid consumed (mL/kg)	av metal ingested day 15−28 (mmol metal/kg day)
normal/H_2O	4	148 ± 48^b	93 ± 8^b	371 ± 17^c	89 ± 2^b	93 ± 20	NA[d]
diabetic/H_2O	4	1874 ± 369	224 ± 30	250 ± 10	403 ± 17	965 ± 42	NA[d]
diabetic/K_2[(Codipic)$_2$]	8	654 ± 145^b	115 ± 9^b	204 ± 10	340 ± 13	633 ± 28	1.41 ± 0.04
diabetic/$VOSO_4$	7	212 ± 26^b	75 ± 3^b	227 ± 30	262 ± 67	258 ± 62	0.66 ± 0.03

[a] The procedures for induction of diabetes and animal care are described in the Experimental Section. The drinking solution for the animals treated with $VOSO_4$ contained on average 0.78 mg/mL (3.1 mM) for days 1−14 and for the animals treated with $[Co(dipic)_2]^{2-}$ contained 0.50 mg/mL (0.84 mM) for days 1−3 and 0.60 mg/mL (1.01 mM) for days 4−14. Details for the final 2 weeks of treatment of the selected animals are described in the table. [b] Indicates $p < 0.001$ compared to diabetic. [c] $p < 0.01$. [d] NA = not applicable.

weight is one measure of toxicity. These data suggest that $[Co(dipic)_2]^{2-}$ interferes less with the metabolism of the animal than $VOSO_4$, particularly because the $[Co(dipic)_2]^{2-}$ treated animals ingested twice as much metal as the $VOSO_4$ treated animals. The effect of the dipic ligand on toxicity was also tested on three diabetic animals. These animals consumed 2.62 ± 0.06 mmol/kg day of ligand. The elevated blood glucose levels of the dipic treated animals were not significantly lowered at any time point, and these animals maintained their weight of approximately 200 g throughout the time period (data not shown).

$VOSO_4$ is known to reduce elevated serum triglyceride and cholesterol associated with STZ-induced diabetes.[41] Serum lipid analyses were carried out on four groups of animals (normal, diabetic, $[Co(dipic)_2]^{2-}$ treated, and $VOSO_4$ treated) randomly selected from three experiments of animals administered placebo, $[Co(dipic)_2]^{2-}$, and $VOSO_4$ (see Experimental Section). Data concerning blood glucose levels and body weight at sacrifice, along with metal ingestion, averaged over the final 2 weeks of this 4 week treatment period, is given in Table 5. At the end of 4 weeks of treatment, the Co treated animals chosen for lipid analysis did not show statistically significantly lowering of blood glucose.

The diabetic animals showed increased levels of both triglyceride and cholesterol compared to normal after 4 weeks of treatment. The $VOSO_4$ treated diabetic animals in this experiment show serum lipids lowered to the normal levels ($p \leq 0.001$ vs diabetic) as previously reported.[41] The serum triglycerides and cholesterol levels in the $[Co(dipic)_2]^{2-}$ treated animals were also significantly reduced ($p \leq 0.001$ vs diabetic). The cholesterol levels dropped to near normal levels, while the triglyceride level dropped 3-fold to a level still 4-fold above normal.

Comparison of the Insulin-Like Effects of $K_2[Co(dipic)_2]$ and $VOSO_4$ and Implications of These Studies. Combined, our results show that $[Co(dipic)_2]^{2-}$ had a limited effect on lowering diabetic hyperglycemia and a statistically significant effect on lowering hyperlipidemia without excessive toxicity. This demonstrates that administration of cobalt in a dipicolinato complex can alleviate symptoms of diabetes as has been reported with $CoCl_2$. We observed that $[Co(dipic)_2]^{2-}$ had similar effects as the $CoCl_2$ salt in our system (data not shown). The use of a metal complex allows for greater control of the chemistry of the metal ion and decreases the possibility that the free metal becomes bound to other blood components. Detailed comparisons of the effectiveness of metal complexes in alleviation of the symptoms of diabetes with their chemical profiles, as determined in this paper for $[Co(dipic)_2]^{2-}$, need to be performed. Although only a limited effect is observed on hyperglycemia with $[Co(dipic)_2]^{2-}$ treatment, a potent effect on diabetic hyperlipidemia was observed and is likely to be of mechanistic importance.

The current study was conducted not only to examine the insulin-like effect of $[Co(dipic)_2]^{2-}$ but also to initiate a systematic insulin-like comparison of different metal complexes. No comparisons among metal complexes of insulin-like effects in the same experiment have been reported, but such studies are very important aspects of compound evaluation. Our study involved $[Co(dipic)_2]^{2-}$ and a vanadium salt ($VOSO_4$). At this time, $VOSO_4$ is the best positive control compound, because much is known about this salt in many animal and human systems. Our data show that, at the doses used in this experiment, the hyperglycemia lowering effects of $[Co(dipic)_2]^{2-}$ are less than those of $VOSO_4$. $[Co(dipic)_2]^{2-}$ and $VOSO_4$ are both very effective in lowering elevated serum lipid levels, and this effect may accordingly be related to properties common for the two metal ion complexes. $[Co(dipic)_2]^{2-}$ and $VOSO_4$ did not significantly affect body weight in this experiment; however, this benefit is offset by the lower effect on hyperglycemia. At this time, the origin of the effect of $[VO_2dipic]^-$ on hyperglycemia not observed with $[Co(dipic)_2]^{2-}$ is not clear. Because it is unlikely that $[VO_2(dipic)]^-$ remains unchanged at cellular pH, it has been proposed that this form of the compound is important for transport into the cells containing the biological target. There is no doubt that the redox properties of these complexes are very different and may also be important to these observed biological properties (unpublished). Further studies are necessary to better evaluate and compare the effects of $[Co(dipic)_2]^{2-}$ to those of a corresponding vanadium complex for further insight into effectiveness and whether the lability is important to the effects on hyperlipidemia.

Summary. The synthesis and characterization of Co(II) and Co(III) 2,6-pyridinedicarboxylate ($dipic^{2-}$) have led to solid-state X-ray characterizations performed on [Co(H_2-

(41) Ramanadham, S.; Mongold, J. J.; Brownsley, R. W.; Cros, G. H.; McNeill, J. H. *Am. J. Physiol.* **1989**, *257*, H904−H910.

dipic)(dipic)]·$3H_2O$ and [Co(dipic)(μ-dipic)Co(H_2O)$_5$]·$2H_2O$. Two new coordination modes are observed; one involves metal coordination to the short C−O (C═O) bond, and the other involves metal coordination to a protonated oxygen atom. Solution studies show that several species can exist. In contrast to K[Co(dipic)$_2$], the $[Co(dipic)_2]^{2-}$ complex has pH dependent lability and in this regard is similar to the $[VO_2dipic]^-$ complex.

Acknowledgment. We thank the American Diabetes Foundation for funding this work.

Supporting Information Available: VT-^{1}H NMR spectra for solution containing $[Co(II)(dipic)_2]^{2-}$ and $[Co(III)(dipic)_2]^-$ and solution of [Co(II)(dipic)(μ-dipic)(Co(II)(H_2O)$_5$]·$2H_2O$ (PDF). X-ray crystallographic file (CIF). This material is available free of charge via the Internet at http://pubs.acs.org.

IC020062L